Protein Adsorption Behavior on the Surface of the Microfiltration Membrane Based on a Quartz Crystal Microbalance (QCM)

Zhou Wang[1], Yadong Kong[2], Qian Zhang[2], Zhan Wang[2,*], Natsagdorj Khaliunaa[2], Rooha Khurram[2], Yuenan Zhou[2], Tungalagtamir Bold[3] and Khan Bushra[2]

[1]*Civil engineering, College of Architecture & Civil Engineering, Beijing University of Technology, Beijing 100124, P. R. China*

[2]*Beijing Key Laboratory for Green Catalysis and Separation, College of Environment and Energy Engineering, Beijing University of Technology, Beijing 100124, P.R. China*

[3]*Department of Chemical Enjineering, Mongolian University of Science and Technology, Ulaanbaatar, Mongolia, 14191*

Abstract: How to fast and efficiently determinate the fouling behavior of the microfiltration membrane has great significance for the industrial membrane application. In this paper, the MF membrane was put on the surface of a gold-coated quartz crystal of QCM to study the adsorption behavior of protein at different conditions. The adsorbed mass increased with the increasing of concentration, ionic strength and temperature while decreased with the increasing of pH. Then the BSA adsorption results were compared with the corresponding membrane flux in dead-end cell at the identical conditions. Furthermore, the BSA adsorption process can be described by Langmuir and Freundlich isotherms very well. These results suggested that directly putting the membrane on the surface of a gold-coated quartz crystal of QCM can be used as a rapid and efficient approach to study protein fouling on the membrane surface. This approach using QCM and a small piece of the membrane could yield quantitative information for adsorption kinetics investigation and reduce the workload in large-scale industrial project.

Keywords: Static Adsorption, QCM, Microfiltration Membrane, Isotherm Models.

1. INTRODUCTION

Currently, membrane fouling is an unavoidable phenomenon restricting the wide applications of the membrane technology for water purification and wastewater treatment [1-3].Adsorption has been considered to be the most serious and responsible factor resulting in membrane fouling [4, 5]. Therefore, it is of great significance to study the static adsorption of main foulants. As reported, the extracellular polymeric substances (EPS) are the major substances for membrane fouling in membrane bioreactors (MBR)[6-11]. However, the complexity of extracted EPS in real MBR systems and scarce knowledge of the interactions between EPS and membrane materials force researchers to use model EPS solutions (BSA, Collagen-I and Fibrinogen etc.)[12-17].

The optimization of operating conditions is also an indispensable part for studying adsorption behavior in MBR [18-19]. For example, the amount of BSA adsorbed on the membrane surface was increased with the decreasing of pH value [20] and the rising of temperature [21, 22]. Moreover, the hydrophobic and electrostatic interactions between various sulfonated polystyrene microspheres were also investigated [11, 23]. But the measurement of traditional static adsorption experiments was not continuous and time-consuming [12-16, 20, 21]. Therefore, finding a quick and simple method to monitor the fouling behavior of protein was urgent.

Since the first report in 1972 [24, 25], QCM, based on the piezoelectric effect [26], has been widely applied as a real-time monitor to record the dynamic adsorption behaviors of macromolecular proteins such as immune globulin [27], albumin[28], fibrinogen and so on[29]. And recent attention focuses on the interactions between proteins and membrane surfaces [30-32] as well as the viscoelastic properties of foulants on the membrane surfaces [33, 35]. For example, the deposition mass of hemoglobin-octadecyl amine on a gold surface of QCM was investigated [36]. The thickness of albumin adsorption layer in the Ti-O film surface can be obtained [29]. The morphological and cytoskeletal changes of cells [37, 38] had a great influence on adhesion to the material surface. The QCM can also monitor the changes in amount of macromolecules on the cell surface [39].

However, up to date, the experiments were conducted directly on a gold-coated quartz crystal or on the surface of the membrane which is coated on a

*Address correspondence to this author at the Beijing Key Laboratory for Green Catalysis and Separation, College of Environment and Energy Engineering, Beijing University of Technology, Beijing 100124, P.R. China;
Tel: 86-10-67396186; Fax: +861067391983; E-mail: wangzh@ bjut.edu.cn

E-ISSN: 2409-983X/18

quartz crystal. The quantitative studies about putting membrane on the surface of a gold-coated quartz crystal of QCM haven't been reported yet. Therefore, this study focuses on putting the membrane on the quartz crystal surface of QCM to measure the adsorption behaviors of proteins on MF membranes at different operating conditions (pH, ionic strength, feed concentration and temperature).

2. MATERIALS AND METHODS

2.1. MATERIALS

In the static adsorption experiments, 0.1 μm hydrophilic polyvinylidene fluoride (PVDF), polyacrylonitrile (PAN) and polyether sulfones (PES) microfiltration membranes (ANDE Membrane Separation Technology & Engineering, Beijing CO., Ltd) were used. BSA (Beijing Aoboxing Bio-tech CO., Led) with isoelectric point (IEP) in the range of 4.7 - 4.9 and molecular weight of 67 kDa, Collagen-I (Sigma – Aldrich CO., Led) with IEP in the range of 4.6 - 4.7 and molecular weight of 161 kDa and Fibrinogen (Sigma – Aldrich CO., Led) with IEP in the range of 3.4 - 3.5 and molecular weight of 340 kDa were chosen as model protein. $Na_2HPO_4{\cdot}12H_2O$, $C_6H_8O_7$ and KH_2PO_4 (Beijing YILI fine Chemical Engineering, Ltd.) were used as the preparation of phosphate-buffered solutions (PBS). The ionic strengths were controlled with sodium chloride (NaCl). All chemicals used in this study were of analytical grade. QCM 200 (Stanford Research System, Inc., USA) with AT-cut 5 MHz gold-coated quartz crystal was used to monitor the protein adsorption process.

2.2. Experimental Procedure

2.2.1. Membrane Fouling Experiment using QCM

Before each experiment, all the membranes were cut into wafers with effective surface area of 5.72 cm^2. Then the membrane sample was soaked in DI-water for 10 h to remove protectant (glycerin). The experiments were conducted as follows: (i) the crystal was cleaned by immersed into a solution of 30% hydrogen peroxide/25% ammonia/DI-water (1:1: 5 , V/V/V) and then dried; (ii) Membrane sample (the smooth side outward) was directly put (not coated) on the surface of a gold-coated quartz crystal of QCM and then installed the crystal holder head, thus it was connected to 5 MHz crystal BNC connector of the QCM25 crystal oscillator. Prior to protein adsorption, a stable baseline response of a quartz crystal in air was established (for every test). The absolute frequency was close to 5 MHz; (iii) immersed this quartz crystal into phosphate buffer solution (PBS) to establish initial baseline. After a stable baseline of PBS, this quartz crystal was immersed into protein solution with certain concentration, pH or ionic strength until the adsorption equilibrium was reached. QCM system was employed to monitor continuously the process of the protein mass adsorbed on the surface of the microfiltration membrane as a function of operating time. The adsorbed mass per unit area (Δm) of protein on the membrane surface can be obtained [40, 41]:

$$\Delta m = \Delta f \times \frac{C}{n} \tag{1}$$

where C (17.7 ng·cm^2·Hz^{-1} at $f_{n=1}$ = 5 MHz) was the mass sensitivity constant of the quartz crystal and n was the frequency overtone number (n = 1, 3, …).

2.2.2. Membrane Fouling Experiment in Dead-End Cell

Before each experiment, all the membranes were cut into wafers with effective area of 24.19 cm^2 and after that the membrane sample was soaked in DI-water for 10 h to remove protective agent (glycerin). Then, the membrane sample was soaked in protein solution for 24 h. After fouling test, the pure water flux of the membrane was measured in a dead-end cell at temperature of 20 °C and TMP of 0.04 MPa:

$$J = \frac{\mathrm{d}V}{A \cdot dt} \tag{2}$$

where J is the pure water flux of the membrane, $m^3/(m^2{\cdot}s)$; V is the permeate volume of water obtaining at time t, m^3; A is the effective area of the membrane, m^2.

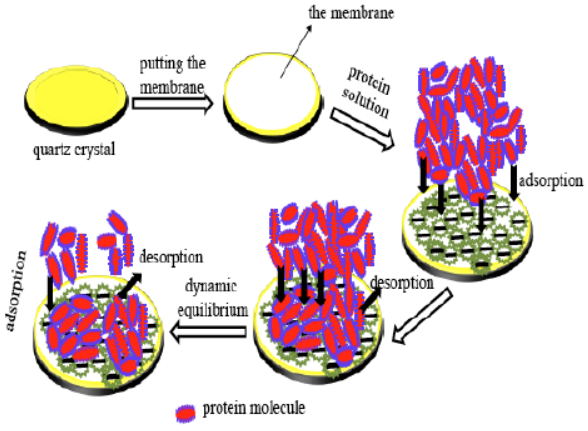

Figure 1: Schematic illustration showing the fouling behavior of proteins deposited on the membrane surface using QCM (put the membrane on the surface of a gold-coated quartz crystal).

Therefore, the fouling behavior of proteins on the surface of the membrane or a quartz crystal was shown in Figure **1**.

2.2.3. Thermodynamic Equation of Adsorption

In the adsorption process, thermodynamic parameters such as enthalpy change ($\Delta_r H^\theta$), entropy change ($\Delta_r S^\theta$) and free energy change ($\Delta_r G^\theta$) were obtained at different temperatures. Then the activation energy (E_a) can be calculated.

$$K = \frac{C_i - C_e}{C_e} \tag{3}$$

$$\Delta_r G^\theta = -RT\ln(K) \tag{4}$$

$$\Delta_r G^\theta = \Delta_r H^\theta - T\Delta_r S^\theta \tag{5}$$

$$\ln(K) = -\frac{E_a}{RT} + \ln A \tag{6}$$

$$\ln(K) = \frac{\Delta_r S^\theta}{R} - \frac{\Delta_r H^\theta}{RT} \tag{7}$$

where K is equilibrium constant. C_e is the equilibrium concentration of BSA in aqueous solution (mg/L), $\Delta_r G^\theta$ is the standard Gibbs free energy (J/mol), $\Delta_r H^\theta$ is the standard enthalpy (J/mol) and $\Delta_r S^\theta$ is the standard entropy (J/(mol·K)).

3. RESULTS AND DISCUSSION

3.1. The static Adsorption of BSA at Different Operating Conditions (put the Membrane on the Surface of a Quartz Crystal of QCM)

As an indicator of membrane fouling, the fundamental understanding of static adsorption mass of protein on the membrane surface at different operating conditions is essential [42]. The pH [43], ionic strength [44], BSA concentration [45] and temperature [46] played an important role in the adsorption process. Therefore, a series of experiments of the static adsorption of BSA on the PVDF membrane surface with pore size of 0.1 μm at different operating conditions were conducted. The adsorbed mass curve declined quickly in the initial followed by a slower drop and then kept stable finally. The initial rapid decline might attribute to concentration polarization and its further reduction caused by the accumulation of the BSA on the membrane surface [47]. A steady stage was reached finally because of further deposition and/or the consolidated layer [48]. The adsorbed mass increased with the increasing of feed concentration, ionic strength and temperature while decreased with the increasing of pH value.

The overall tendency of adsorbed mass (Δm) at different pHs was $\Delta m_{\text{pH=3}}$ (1.71 μg/cm^2) > $\Delta m_{\text{pH=4.92}}$ (0.90 μg/cm^2) > $\Delta m_{\text{pH=6.24}}$ (0.09 μg/cm^2) (Figure **2**(**a**)). This means that the largest adsorption mass was observed at pH 3.0. This could be explained by electrostatic interaction between the membrane surface and BSA molecules [49-51]. The electrostatic repulsion at pH =6.24 resulted in lower adsorbed mass (Δm) [52] while the electrostatic attraction at pH = 3.0[53] resulted in higher adsorbed mass (Δm).

The sequence of the adsorbed mass (Δm) at different ionic strengths was $\Delta m_{\text{I=0.1}}$ (1.25 μg/cm^2) > $\Delta m_{\text{I=0.01}}$ (1.10 μg/cm^2) > $\Delta m_{\text{I=0}}$ (0.09 μg/cm^2) (Figure **2**(**b**)). The reason may be following: when pH value is close to isoelectric point (IEP), more adsorbed mass on the membrane was observed due to the fact that protein is an amphoteric electrolyte with the least electrostatic repulsion and solubility at IEP [41].

The sequence of adsorbed mass at different BSA concentrations (Δm) was $\Delta m_{\text{C=2000 mg/L}}$ (2.71 μg/cm^2) > $\Delta m_{\text{C=1000 mg/L}}$ (2.28 μg/cm^2) > $\Delta m_{\text{C=800 mg/L}}$ (1. 90 μg/cm^2) > $\Delta m_{\text{C=500 mg/L}}$ (1.08 μg/cm^2) (Figure **2**(**c**)). In addition, the increasing of BSA concentration created stronger interactions between BSA solution and the PVDF membrane surface and higher viscosity [54]. This will result in more adsorbed mass on the membrane and more serious membrane fouling.

The sequence of adsorbed mass (Δm) at different temperatures was $\Delta m_{\text{T=310K}}$ (6.34 μg/cm^2) > $\Delta m_{\text{T=300K}}$ (3.32 μg/cm^2) > $\Delta m_{\text{T=290K}}$ (0.90 μg/cm^2) (Figure **2**(**d**)). The unfolding structure of BSA molecule at higher temperature weakened the electrostatic repulsion between BSA molecules and the membrane surface [55] and strengthened the hydrophobic interactions between BSA molecules [56]. Consequently, the process of BSA absorption on the membrane surface was accelerated. Consequently, a higher rate of aggregation occurred.

In summary, the adsorbed mass of BSA on the PVDF membrane surface (put on the surface of a quartz crystal of QCM) increased with the increasing of BSA concentration, ionic strength and temperature while decreased with the increasing of pH value.

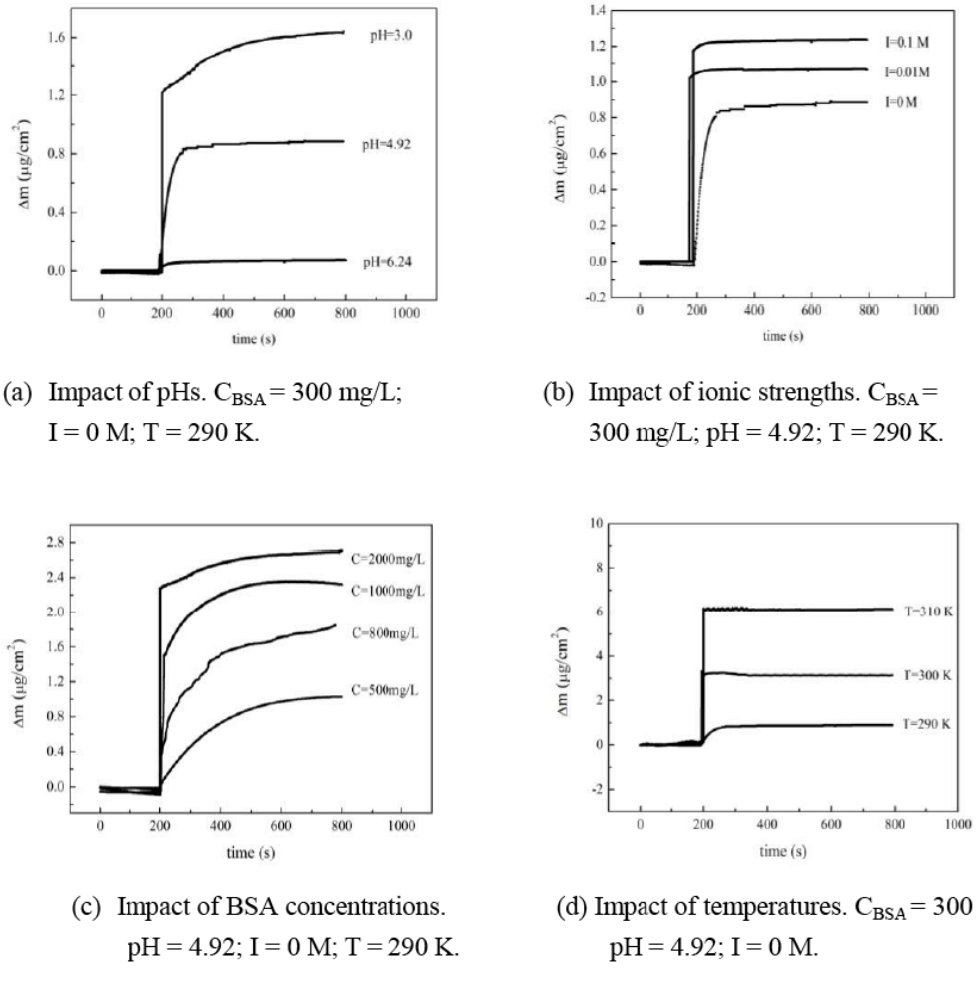

(a) Impact of pHs. C_{BSA} = 300 mg/L; I = 0 M; T = 290 K.

(b) Impact of ionic strengths. C_{BSA} = 300 mg/L; pH = 4.92; T = 290 K.

(c) Impact of BSA concentrations. pH = 4.92; I = 0 M; T = 290 K.

(d) Impact of temperatures. C_{BSA} = 300 mg/L; pH = 4.92; I = 0 M.

Figure 2: The variation of $\triangle m$ during the exposure of the PVDF membrane (put on the surface of a quartz crystal) to PBS and then BSA solution at different operating conditions.

3.2. The Static Adsorption of Different Proteins on Different Microfiltration Membranes (put the Membrane on the Surface of a Gold-Coated Quartz Crystal of QCM)

In order to validate the conclusion obtained in above, the other microfiltration membranes (0.1 μm PAN and PVDF flat-sheet membranes) and the other proteins (Collagen-I and Fibrinogen) were selected to study the protein fouling behavior on the membrane surface (C = 300 mg/L; I = 0 M; T = 290 K).

Firstly, the absorbed mass of Fibrinogen had a rapid increase trend than that of BSA and Collagen-I (Figure **3**(**a**)). The sequence of adsorbed mass (Δ*m*) was $\Delta m_{Fibrinogen}$ (3.43 μg/cm^2) > $\Delta m_{Collagen\text{-}I}$ (0.89 μg/cm^2) > Δm_{BSA} (0.75 μg/cm^2). This may be attributed to the fact that fibrinogen has a higher activity at the solid-liquid interfaces than that of other proteins [57, 58] . The adsorbed mass of BSA is less than that of Collagen-I might due to the difference in their molecular size [59].

Secondly, the sequence of BSA adsorbed mass (Δm) on the surface of different microfiltration membranes was Δm_{PES} (0.75 μg/cm^2) > Δm_{PVDF} (0.69 μg/cm^2) > Δm_{PAN} (0.25 μg/cm^2) (Figure **3**(**b**)). This because the adsorbed mass of BSA on the membrane surface was inversely proportional to the hydrophilic of the membrane [60, 61] and the higher hydrophobicity of the membrane surface caused the more serious fouling [62]. As measured, the contact angle of PES, PVDF and PAN was 77.3 ± 4.85º, 69.6 ± 2.24º and 63.9 ± 3.32º, respectively. Therefore, the sequence of adsorbed mass (Δ*m*) was $\Delta m_{PES} > \Delta m_{PVDF} > \Delta m_{PAN}$.

Based on the above discussion in the section 3.2, we can draw the conclusion that the static adsorption behavior of 0.1 μm PVDF, PAN and PES MF membranes using BSA, Collagen-I and Fibrinogen were kept a similar trend when the tested membrane was put on the surface of a quartz crystal of QCM.

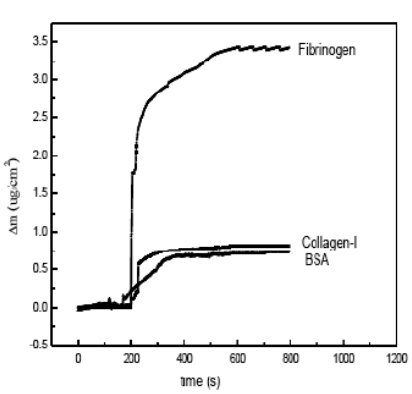

(a) PVDF membrane. C_i = 300 mg/L; I = 0 M; T = 290 K.

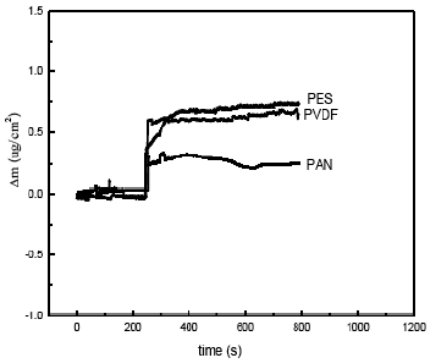

(b) BSA solution. C_i=300 mg/L; I = 0 M; T = 290 K.

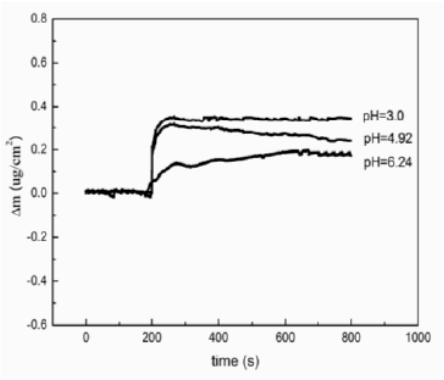

(c) Impact of pHs (only quartz crystal without membrane). C_{BSA} = 300 mg/L; I = 0 M; T = 290 K.

Figure 3: The variation of $\triangle m$ during the exposure of membrane to PBS and then protein solution using QCM.

3.3. The Validation Experiments of Protein Adsorption on a Quartz Crystal Surface of QCM or on the Membrane Surface in Dead-End Cells

Firstly, the absorbed mass on a quartz crystal surface had a similar but relatively gentle trend with that when membrane was put on the surface of a quartz crystal (Figure **3**(**c**)). The variation of adsorbed mass (Δm) was $\Delta m_{pH=3}$ (0.35 μg/cm^2) > $\Delta m_{pH=4.92}$ (0.24 μg/cm^2) > $\Delta m_{pH=6.24}$ (0.18 μg/cm^2). This might mainly result from the electrostatic interaction force between BSA and a quartz crystal was weaker.

Secondly, the pure water flux (PWF) of PVDF membranes fouled with BSA solution for 24 h were tested in dead end cell. PWF of the membrane decreased with the decreasing of pH value (Figure **4**(**a**)). The more BSA mass was adsorbed, the lower PWF was [63]. Therefore, the corresponding variation of PWF (J) was $J_{pH=6.24}$ (1.59 m^3/(m^2·s)) > $J_{pH=4.92}$ (1.37 m^3/(m^2·s)) > $J_{pH=3}$ (0.18 m^3/(m^2·s)).

Thirdly, when achieving BSA adsorption equilibrium at different ionic strengths (I = 0, 0.01 and 0.1) in dead-end cell, the corresponding PWF increased with the decreasing of ionic strength (Figure **4**(**b**)) as reported by other researchers [63]. The corresponding variations of J was $J_{I=0}$ (1.15 m^3/(m^2·s)) > $J_{I=0.01}$ (1.08 m^3/(m^2·s)) > $J_{I=0.1}$ (0.89 m^3/(m^2·s)).

In summary, it was clear that the adsorption behavior of BSA on the membrane surface (put on the surface of a gold-coated quartz crystal) (Figure **2a**) is more serious than that only on the surface of a quartz crystal (Figure **3c**) at different pH levels. And the result of Figure **2**(**a**) and Figure **2**(**b**) is consistent with PWF (J) obtained from dead-end filtration experiments (Figure **4**). Therefore, QCM (putting the membrane on the surface of a gold-coated quartz crystal) can be used to monitor the actual static adsorption behavior of BSA on the surface of PVDF membrane at different ionic strengths.

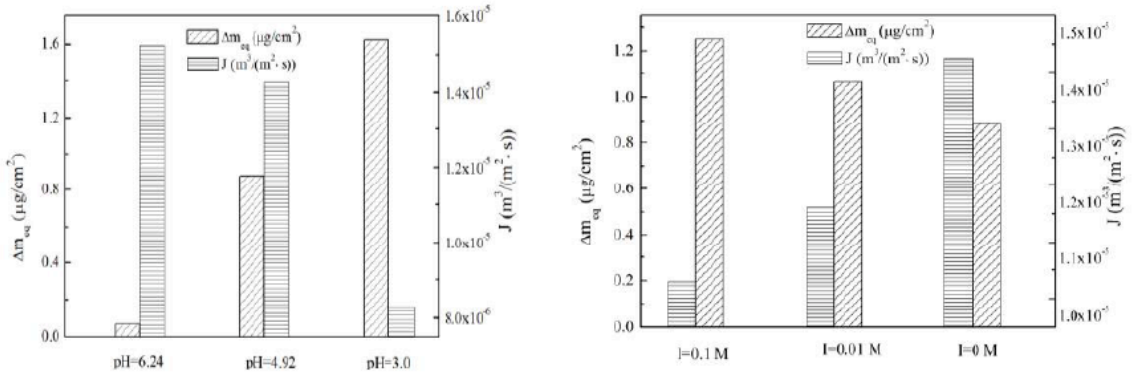

(a) at different pHs. C_{BSA} = 300 mg/L; I = 0 M; T = 290 K.

(b) at different ionic strengths. C_{BSA} = 300 mg/L; pH = 4.92; T = 290 K.

Figure 4: The comparison of BSA adsorbed mass at equilibrium on the PVDF membrane surface using QCM with the corresponding PWF obtained in dead-end cell.

3.4. Isotherm Models and Thermodynamic Parameters

It is also important to select the most appropriate isotherm model for the equilibrium curve to evaluate the applicability of the sorption process of BSA on the membrane surface. Four different adsorption isotherms in Table **1** were used to describe the experimental result at 290 K. The nonlinear error functions in Table **2** (R^2, SSE, RMSE, and Chi-Square) were discussed to gauge the goodness-of-fit.

Comparatively speaking, the sequence of R^2 values were 0.99 (Langmuir and Freundlich) > 0.97 (BET) > 0.96 (Langmuir) > 0.94 (Freundlich). On the contrary, the value of SSE, RMSE, and Chi-Square for Langmuir

Table 1: The Presentation of Four Different Isotherms and their forms

No	Name	Isotherm Model	Description for Constants and Parameters
1	Langmuir isotherm	$\Gamma = \frac{K_L Q_m C_e}{1 + K_L C_e}$	Γ is the adsorption capacity at equilibrium (μg/g); K_L is constant associated with the energy of adsorption; Q_m is the maximum adsorption capacity of BSA on PVDF membrane (μg/g); C_e is the equilibrium concentration of BSA in aqueous solution (mg/L)
2	Freundlich isotherm	$\Gamma = K_F C_e^{\frac{1}{n}}$	K_F is constant which represents adsorption capacity; n is parameter which indicates adsorption intensity.
3	Langmuir and Freundlich isotherm	$\Gamma = Q_m \frac{(K_{LF} C_e)^{\frac{1}{n}}}{1 + (K_{LF} C_e)^{\frac{1}{n}}}$	K_{LF} is constant.
4	BET isotherm	$\Gamma = Q_m \frac{K_{BET1} C_e}{(1 - K_{BET2} C_e)(1 - K_{BET2} C_e + K_{BET1} C_e)}$	K_{BET1} and K_{BET2} are constants.

Table 2: Nonlinear Regression Parameters for fit of BSA Adsorption (put the Membrane on the Surface of a Gold Coated Quartz Crystal, pH=4.92, I=0, T=290K)

Isotherms	R^2	RMSE	Chi-Square	SSE
Langmuir	0.96	14.33	4.22	1026.4
Freundlich	0.94	17.79	6.36	1583.1
Langmuir and Freundlich	0.99	3.07	0.16	47.02
BET	0.97	12.90	3.59	832.3

and Freundlich adsorption isotherms was smallest (47.02, 3.07, and 0.16, respectively). In addition, Freundlich was validated as the most unsuccessful prediction with the highest values of SSE, RMSE and Chi-Square (1583.1, 17.79, and 6.36, respectively). Therefore, Langmuir and Freundlich isotherms were the most suitable to fit the experimental data for the adsorption of BSA on the membrane surface at 290 K. The best-fitting model curve presented in Figure **5**, a steep rise in the initial period was observed and then it became gentle. Therefore, the curves were considered as the L-type. Besides, the similar result had been acquired about the adsorption behavior of BSA on the surface of hydrophilic polyether sulfone (PES) MF membrane [21] and of anion polyacrylamide on the PVDF UF membrane surface [64].

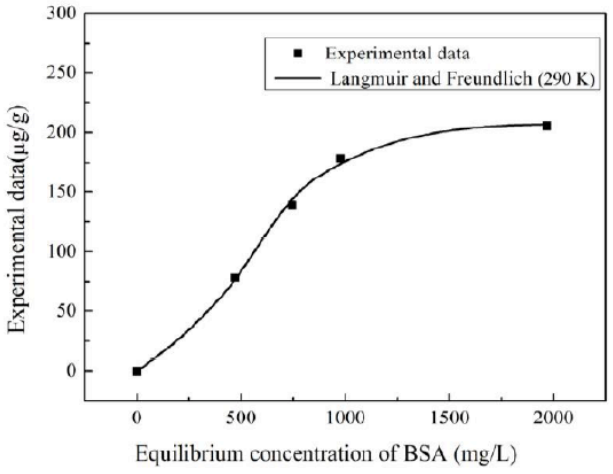

Figure 5: The best-fitting adsorption isotherm (Langmuir and Freundlich) for BSA adsorption on the surface of the PVDF membrane using QCM. The test condition of: C_{BSA} = 500, 800, 1000 and 2000 mg/L; pH = 4.92; I = 0 M; T = 290 K.

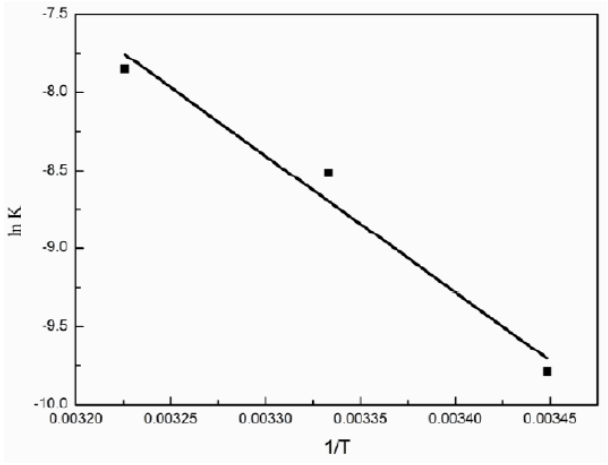

Figure 6: Van't Hoff plots of BSA adsorption on the PVDF membrane surface for different temperatures using QCM. The condition of BSA solution: T = 290, 300 and 310 K; C_{BSA} = 300 mg/L; pH = 4.92; I = 0 M.

The values of standard Gibbs free energy ($\Delta_r G^\theta$) at 290, 300 and 310 K were 23.40, 21.69 and 19.99 kJ/mol, respectively. These values were all positive, which indicates that the process of BSA absorption on the membrane surface was feasible but not spontaneous. In addition, the $\Delta_r G^\theta$ value decreased as the temperature increased. This means that the increasing of temperature would accelerate the process of BSA absorption. The values of $\Delta_r H^\theta$ and $\Delta_r S_\theta$ were also obtained from the slope and intercept of the plot of ln (K) versus 1/T (Figure **6**). The value of $\Delta_r H^\theta$ was 72.72 kJ/mol, the positive value manifested that the process of BSA absorption was endothermic [65]. Here, the positive activation energy (E_a=72.72 kJ/mol) also indicated that the process of BSA absorption was endothermic [22]. The value of $\Delta_r S^\theta$ was 170 J/(K·mol), the positive value reflects that the distribution of the adsorption of BSA on the PVDF membrane surface was more chaotic than that in the aqueous solution, maybe this is due to the interaction between the membrane and BSA molecules[66].

CONCLUSION

In this paper, the fouling behaviors of different proteins on the different microfiltration membranes (put on the surface of a gold-coated quartz crystal of QCM) were systemically studied at different operating conditions (pHs, ionic strengths, concentrations and temperatures). The protein adsorbed mass increased with the increasing of protein concentration, ionic strength and temperature while decreased with the increasing of pH value. And the best-fitted adsorption isotherm model was Langmuir and Freundlich for the process of BSA adsorption, which was endothermic and not spontaneous. The obtained adsorption mass was also compared with that obtained only on the surface of a gold-coated quartz crystal and the corresponding permeate flux of the membrane at the identical operating condition in dead-end cell. The experimental results show that the fouling behaviors of different proteins on other 0.1 μm microfiltration membranes keep the similar trend. Therefore, QCM provide an easy, fast and effective way for monitoring protein adsorption on the membrane surface which is directly put on the surface of a gold-coated quartz crystal of QCM. This approach using a small piece of the membrane would decrease the work load as well as the energy consumption in industrial process.

ACKNOWLEDGEMENTS

Support for this work was provided by National Natural Science Foundation of China (project no. 21176006 and 21476006).

NOMENCLATURE

A the effective area of the membrane (m^2)

C the mass sensitivity constant of the quartz crystal

C_e the equilibrium concentration of BSA in aqueous solution (mg/L)

C_i the using concentration of BSA in aqueous solution (mg/L)

E_a activation energy(kJ/mol)

Δf frequency shift (MHz)

$\Delta_r G^\theta$ standard Gibbs free energy (J/mol)

$\Delta_r H^\theta$ standard enthalpy (J/mol)

I the ionic strength of the protein solution

J the pure water flux (m^3/ (m^2·s))

K_{BET} constant

K_F constant which represents adsorption capacity

K_L constant associated with the energy of adsorption

K_{LF} constant

Δm adsorbed mass per unit surface

n the frequency overtone number

n parameter which indicates adsorption intensity

Q_m the maximum adsorption capacity of BSA on PVDF membrane (μg/g)

$\Delta_r S^\theta$ standard entropy (J/(mol·K))

T the temperature of the protein solution

V the permeate volume of water obtaining at time t (m^3)

Γ the adsorption capacity at equilibrium (μg/g)

REFERENCES

[1] Y. Miura, Y. Watanabe, S. Okabe, Membrane fouling in pilot-scale membrane bioreactors (MBRs) treating municipal wastewater: Impact of biofilm formation, Environ. Sci. Technol. 41 (2007) 632-638. https://doi.org/10.1021/es0615371

[2] S.G. Yiantsios, A.J. Karabelas, An experimental study of humic acid and powdered activated carbon deposition on UF membranes and their removal by backwashing, Desalination 140 (2001) 195-209. https://doi.org/10.1016/S0011-9164(01)00368-X

[3] K. Kimura, N. Yamato, H. Yamamura, Y. Watanabe, Membrane biofouling in pilot-scale membrane bioreactors (MBRs) treating municipal wastewater, Environ. Sci. Technol. 39 (2005) 6293-6299. https://doi.org/10.1021/es0502425

[4] K. Katsoufidou, S.G. Yiantsios, A.J. Karabelas, An experimental study of UF membrane fouling by humic acid and sodium alginate solutions: the effect of backwashing on flux recovery, Desalination 220 (2008) 214-227. https://doi.org/10.1016/j.desal.2007.02.038

[5] F., Meng, S.R. Chae, A., Drews, M. Kraume, H.S. Shin, F. Yang, 2009. Review: recent advances in membrane bioreactors (MBRs): membrane fouling and membrane material, Water Res. 43 (2009) 1489-1512. https://doi.org/10.1016/j.watres.2008.12.044

[6] M.F. Dignac, V. Urbain, Chemical description of extracellular polymers: implication on activated sludge floc structure, Water Sci. Technol. 38 (1998) 45-53. https://doi.org/10.2166/wst.1998.0789

[7] B. Frølund, T. Griebe, P.H. Nielsen, Enzymatic activity in the activated-sludge floc matrix, Appl. Microbiol. Biot. 43 (1995) 755-761. https://doi.org/10.1007/s002530050481

[8] B. FrØlund, R. Palmgren, Extraction of extracellular polymers from activated sludge using a cation exchange resin. Water Res. 30 (1996) 1749-1758. https://doi.org/10.1016/0043-1354(95)00323-1

[9] [9] J.I. Houghton, T. Stephenson, Effect of influent organic content on digested sludge extracellular polymer content and dewater ability, Water Res. 36 (2002) 3620-3628. https://doi.org/10.1016/S0043-1354(02)00055-6

[10] S. Tsuneda, S. Park, Enhancement of nitrifying biofilm formation using selected EPS produced by heterotrophic bacteria, Water Sci. Technol. 43 (2001) 197-204. https://doi.org/10.2166/wst.2001.0374

[11] J.Y. Yoon, J.H. Kim, W.S. Kim, Interpretation of protein adsorption phenomena onto functional microspheres, Colloid. Surface. B 12 (1998) 15-22. https://doi.org/10.1016/S0927-7765(98)00045-9

[12] H. Nagaoka, S. Yamanishi, A. Miya, Modeling of biofouling by extracellular polymers in a membrane separation activated sludge system, Water Sci. Technol. 38 (1998) 497-504. https://doi.org/10.2166/wst.1998.0705

[13] S. Ognier, C. Wisniewski, Influence of macromolecule adsorption during filtration of a membrane bioreactor mixed liquor suspension, J. Membr. Sci. 209 (2007) 27-37. https://doi.org/10.1016/S0376-7388(02)00123-0

[14] S. Rosenberger, H. Evenblij, S. Tepoele, T. Wintgens, C. Laabs, The importance of liquid phase analyses to understand fouling in membrane assisted activated sludge Processes-six case studies of different European research groups, J. Membr. Sci. 263 (2005) 113-126. https://doi.org/10.1016/j.memsci.2005.04.010

[15] M. Yao, K. Zhang, L. Cui, Characterization of protein-polysaccharide ratios on membrane fouling, Desalination 259 (2010) 11-16. https://doi.org/10.1016/j.desal.2010.04.049

[16] Y. Ye, P. Le Clech, V. Chen, Fouling mechanisms of alginate solutions as model extracellular polymeric substances, Desalination 175 (2005) 7-20. https://doi.org/10.1016/j.desal.2004.09.019

[17] Y. Ye, P. Le Clech, V. Chen, Evolution of fouling during crossflow filtration of model EPS solutions, J. Membr. Sci. 264 (2005) 190-199. https://doi.org/10.1016/j.memsci.2005.04.040

[18] K. Nakamura, K. Matsumoto, Protein adsorption properties on a microfiltration membrane: a comparison between static and dynamic adsorption methods, J. Membr. Sci. 285 (2006)

126-136.
https://doi.org/10.1016/j.memsci.2006.08.012

[19] H. Susanto, M. Ulbricht, Influence of ultrafiltration membrane characteristics on adsorptive fouling with dextrans, J. Membr. Sci. 266 (2005) 132-142.
https://doi.org/10.1016/j.memsci.2005.05.018

[20] P. Aimar, S. Baklouti, V. Sanchez, Membrane-solute interaction: influence on pure solvent transport during ultrafiltration, J. Membr. Sci. 29 (1986) 207-224.
https://doi.org/10.1016/S0376-7388(00)82470-9

[21] S.M.G. Demneh, B. Nasernejad, H. Modarres, Modeling investigation of membrane biofouling phenomena by considering the adsorption of protein, polysaccharide and humic acid, Colloid. Surface. B. (2011) 108-114.
https://doi.org/10.1016/j.colsurfb.2011.06.018

[22] Y.N. Zhou, Z. Wang, Q. Zhang, X.J. Xi, J. Zhang, W.T. Yang, Equilibrium and thermodynamic studies on adsorption of BSA using PVDF microfiltration membrane, Desalination 307 (2012) 61-67.
https://doi.org/10.1016/j.desal.2012.09.004

[23] J.Y. Yoon, J.H. Kim, W.S. Kim, The relationship of interaction forces in the protein adsorption onto polymeric microspheres, Colloid Surf. A-Physicochem. Eng. Asp. 153 (1999) 413-419.
https://doi.org/10.1016/S0927-7757(98)00533-0

[24] C.G. Marxer, M.C. Coen, L. Schlapbach, Study of adsorption and viscoelastic properties of proteins with a quartz crystal microbalance by measuring the oscillation amplitude, J. Colloid Interface Sci. 261 (2003) 291-298.
https://doi.org/10.1016/S0021-9797(03)00089-4

[25] A.G. Hemmersam, M. Foss, J. Chevallier, F. Besenbacher, Adsorption of fibrinogen on tantalum oxide, titanium oxide and gold studied by the QCM-D technique, Colloid. Surface.B. 43 (2005) 208-215.
https://doi.org/10.1016/j.colsurfb.2005.04.007

[26] Y. Liu, X. Yu, R. Zhao, Quartz crystal biosensor for real-time monitoring of molecular recognition between protein and small molecular medicinal agents, Biosens. Bioelectron. 19 (2003) 9-19.
https://doi.org/10.1016/S0956-5663(03)00127-1

[27] M.S. Lord, M.H. Stenzel, A. Simmons, B.K. Milthorpe, The effect of charged groups on protein interactions with poly (HEMA) hydrogels, Biomaterials 27 (2006) 567-575.
https://doi.org/10.1016/j.biomaterials.2005.06.010

[28] F. Hook, J. Voros, M. Rodahl, A comparative study of protein adsorption on titanium oxide surfaces using in situ ellipsometry, optical waveguide light mode spectroscopy, and quartz crystal microbalance/dissipation, Colloid. Surface. B. 24 (2002) 155-170.
https://doi.org/10.1016/S0927-7765(01)00236-3

[29] F. Yin, S. Park, HK. Shin, Study of hemoglobin-octadecylamine Lb film formation and deposition by compressibility analyse, QCM and AFM. Curr. Appl. Phys. 6 (2006) 728-734.
https://doi.org/10.1016/j.cap.2005.04.028

[30] M.S. Lord, B.G. Cousins, P.J. Doherty, The effect of silica nanoparticulate coatings on serum protein adsorption and cellular response, Biomaterials 27 (2006) 4856-4862.
https://doi.org/10.1016/j.biomaterials.2006.05.037

[31] G.V. Lubarsky, M.R. Davidson, R.H. Bradley, Hydration-dehydration of adsorbed protein films studied by AFM and QCM, Biosens. Bioelectron. 22 (2006) 1275-1281.
https://doi.org/10.1016/j.bios.2006.05.024

[32] X. Chu, Z.L. Zhao, G.L. Shen, Quartz crystal microbalance immunoassay with dendritic amplification using colloidal gold immunocomplex, Sensor. Actuat. B-Chem. 114 (2006) 696-704.
https://doi.org/10.1016/j.snb.2005.06.014

[33] J.S. Kavanaugh, W.F. Moo-Penn, A. Arnone, Accommodation of insertions in helixes: The mutation in hemoglobin catonsville (Pro37. alpha.-Glu-Thr 38. alpha.) generates a 310.fwdarw. alpha. Bulge, Biochemistry 32 (1993) 2509-2513.
https://doi.org/10.1021/bi00061a007

[34] A. Welle, A. Chiumiento, R. Barbucci, Biomolecular Engineering 24 (2006) 87.
https://doi.org/10.1016/j.bioeng.2006.05.027

[35] B. Van der Bruggen, L. Braeken, C. Vandecasteele, Flux decline in nanofiltration due to adsorption of organic compounds, Sep. Purif. Technol. 29 (2002) 23-31.
https://doi.org/10.1016/S1383-5866(01)00199-X'

[36] C. Velasco, J.I. Calvo, L. Palacio, J. Carmona, P. Prádanos, A. Hernández, Flux kinetics, limit and critical fluxes for low pressure dead-end microfiltration. The case of BSA Filtration through a Positively Charged Membrane, Chem. Eng. Sci. 129 (2015) 58-68.
https://doi.org/10.1016/j.ces.2015.02.003

[37] H.P. Chu, X. Li, Membrane fouling in a membrane bioreactor (MBR): sludge cake formation and fouling characteristics, Biotechnol. Bioeng. 90 (2005) 323-331.
https://doi.org/10.1002/bit.20409

[38] K.L. Jones, C.R. O'Melia, Protein and humic acid adsorption onto hydrophilic membrane surfaces: effects of pH and ionic strength, J. Membr. Sci. 165 (2000) 31-46.
https://doi.org/10.1016/S0376-7388(99)00218-5

[39] A. Fane, C. Fell, A. Suki, The effect of pH and ionic environment on the ultrafiltration of protein solutions with retentive membranes, J. Membr. Sci. 16 (1983) 195-210.
https://doi.org/10.1016/S0376-7388(00)81310-1

[40] C.A. Haynes, W. Norde, Globular proteins at solid/liquid interfaces, Colloid. Surface. B. 2 (1994) 517-566.
https://doi.org/10.1016/0927-7765(94)80066-9

[41] M. Hashino, K. Hirami, T. Ishigami, Y. Ohmukai, T. Maruyama, N. Kubota, H. Matsuyama, Effect of kinds of membrane materials on membrane fouling with BSA, J. Membr. Sci. 384 (2011) 157- 165.
https://doi.org/10.1016/j.memsci.2011.09.015

[42] J. Hu, S.J. Li, B.L. Liu, Adsorption of BSA onto sulfonated microspheres, Biochem. Eng. J. 23 (2005) 259-263.
https://doi.org/10.1016/j.bej.2005.01.018

[43] X.M. Yan, J. Kong, C.C. Yang, G.Q. Fu, Facile synthesis of hairy core-shell structured magnetic polymer submicrospheres and their adsorption of bovine serum albumin, J. Colloid Interf. Sci. 445 (2015) 9-15.
https://doi.org/10.1016/j.jcis.2014.12.022

[44] H.J. Mo, K.G. Tay, H.Y. Ng, Fouling of reverse osmosis membrane by protein (BSA): Effects of pH, calcium, magnesium, ionic strength and temperature, J. Membr. Sci. 315 (2008) 28-35.
https://doi.org/10.1016/j.memsci.2008.02.002

[45] U.V. Dortmund, F. Chemie, O.H Strass, O. Hollmann, C. Czeslik, Characterization of a Planar Poly(acrylic acid) Brush as a Materials Coating for Controlled Protein Immobilization, Langmuir 22 (2006) 3300-3305.
https://doi.org/10.1021/la053110y

[46] D. Xu, X.L. Tan, C.L. Chen, X.K. Wang, Adsorption of Pb (II) from aqueous solution to MX-80 bentonite: effect of pH, ionic strength, foreign ions and temperature, Applied Clay Science 41 (2008) 37-46.
https://doi.org/10.1016/j.clay.2007.09.004

[47] C.V. Vidal, A.O. Juan, A.I. Muñoz, Adsorption of bovine serum albumin on CoCrMo surface: Effect of temperature and protein concentration, Colloid. Surface B. 80 (2010) 1-11.
https://doi.org/10.1016/j.colsurfb.2010.05.005

[48] Y.Y. Wang, T. Wang, Y.L. Su, F.B. Peng, H. Wu, Z.Y. Jiang, Remarkable Reduction of Irreversible Fouling and Improvement of the Permeation Properties of Poly(ether sulfone) Ultrafiltration Membranes by Blending with Pluronic

F127, Langmuir 21 (2005) 11856-11862. https://doi.org/10.1021/la052052d

[49] A.D. Marshall, P.A. Munro, G. Trägårdh, The effect of protein fouling in microfiltration and ultrafiltration on permeate flux, protein retention and selectivity: A literature review, Desalination 91 (1993) 65-108. https://doi.org/10.1016/0011-9164(93)80047-Q

[50] Nigam, M.O., Bansal B., Chen X.D, Fouling and cleaning of whey protein concentrate fouled ultrafiltration membranes, Desalination 218 (2008) 313-322. https://doi.org/10.1016/j.desal.2007.02.027

[51] X.S. Yi, W.X. Shi, S.L. Yua, Y. Wang, N. Suna, L.M. Jin, S. Wang, 2011. Isother and kinetic behavior of adsorption of anion polyacrylamide (APAM) from aqueous solution using two kinds of PVDF UF membranes, J. Hazard. Mater. 189 (2011) 495-501. https://doi.org/10.1016/j.jhazmat.2011.02.063

[52] T. Kopac, K. Bozgeyik, J. Yener, Effect of pH and temperature on the adsorption of bovine serum albumin onto titanium dioxide, Colloid Surf. A- Physicochem. Eng. Asp. 322 (2008) 19-28. https://doi.org/10.1016/j.colsurfa.2008.02.010

[53] T. Trongsatitkul, B.M. Budhlall, Temperature dependence of serum protein adsorption in PEGylated PNIPAm Microgels, Colloid Surface B. 103 (2013) 244-252. https://doi.org/10.1016/j.colsurfb.2012.10.053

[54] N. Shamim, L. Hong, K. Hidajat, M.S. Uddin, Thermosensitive-polymer-coated magnetic nanoparticles: Adsorption and desorption of Bovine Serum Albumin, J. Colloid Interface Sci. 304 (2006) 1-8. https://doi.org/10.1016/j.jcis.2006.08.047

[55] C. Veerman, L.M.C. Sagis, J. Heck, E.V.D. Linden, Mesostructure of fibrillar bovine serum albumin gels, Int. J. Biol. Macromol. 31 (2003) 139-146. https://doi.org/10.1016/S0141-8130(02)00074-0

[56] M. Alkan, O. Demirbas, S. Celikcapa, M. Dogan, Sorption of acid red 57 from aqueous solution onto sepiolite, J. of Hazard. Mater. 116 (2004) 135-145. https://doi.org/10.1016/j.jhazmat.2004.08.003

[57] Y.Y. Zuo, R. Gitiafroz, E. Acosta, Z. Policova, P. N. Cox, M.L. Hair, A.W. Neumann, Effect of Humidity on the Adsorption Kinetics of Lung Surfactant at Air-Water Interfaces, Langmuir 21 (2005) 10593-10601. https://doi.org/10.1021/la0517078

[58] N. Chandrasekaran, S. Dimartino, C.J. Fee, Study of the adsorption of proteins on stainless steel surfaces using QCM-D, Chem. Eng. Res. Des. 91 (2013) 1674-1683. https://doi.org/10.1016/j.cherd.2013.07.017

[59] K. C. Dee, D.A. Puleo, R. Bizios, Biomaterials, in An Introduction to Tissue biomaterial interactions, New Jersey, NJ: John Willey and Sons Inc. press. (2002) 165-214. https://doi.org/10.1002/0471270598

[60] A.R. Sarasam, R.K. Krishnswamy, S.V. Madihally, Blending ehitosan with Polycaprolactone: effects on Physicochemical and antibacterial properties, Biornacromoleeules 7 (2006) 1131-1138. https://doi.org/10.1021/bm050935d

[61] L. Feng, J.D. Andrade, Protein adsorption on low temperature isotropic carbon: III. isotherms, competitivity, desorption and exchange of human albumin and fibrinogen, Biomaterials 15 (1994) 323-33. https://doi.org/10.1016/0142-9612(94)90243-7

[62] L. Feng, J.D. Andrade, Structure and adsorption properties of fibrinogen, In Proteins at interfaces II; Horbett T., *et al.*, ACS Symposium Series; American Chemical Society: Washington, DC (1995) 66-79. https://doi.org/10.1021/bk-1995-0602.ch005

[63] M.Q. Zhang, T. Desai, M. Ferrari, Proteins and cells on PEG immobilized silicon surfaces, Biomaterials 19 (1998) 953-960. https://doi.org/10.1016/S0142-9612(98)00026-X

[64] P. Le-Clech, V. Chen, T.A.G. Fane, Fouling in membrane bioreactors used in wastewater treatment, J. Membr. Sci. 284 (2006) 17-53. https://doi.org/10.1016/j.memsci.2006.08.019

[65] J.L.G. Ribelles, Blending polysaccharides with biodegradable Polymers. I. Properties of chitosan/polycaprolactone blends, J. Biomed. Mater. Res. B 85 (2008) 303-313. https://doi.org/10.1002/jbm.b.30947

[66] G.J. Zhang, S.L. Ji, X. Gao, Z.Z. Liu, Adsorptive fouling of extracellular polymeric substances with polymeric ultrafiltration membranes, J. Membr. Sci. 309 (2009) 28-35. https://doi.org/10.1016/j.memsci.2007.10.012

Received on 1-10-2018 Accepted on 22-12-2018 Published on 31-12-2018

DOI: https://doi.org/10.15377/2409-983X.2018.05.2